

Coverage Analysis of Relay Assisted Millimeter Wave Cellular Networks with Spatial Correlation

Simin Xu*, Nan Yang*, Biao He[†], and Hamid Jafarkhani[‡]

*Research School of Electrical, Energy and Materials Engineering,
Australian National University, Canberra, ACT 2601, Australia

[†]MediaTek USA Inc., Irvine, CA 92606, USA

[‡]Center for Pervasive Communications and Computing, University of California, Irvine, CA 92697-2625, USA
Email: simin.xu@anu.edu.au, nan.yang@anu.edu.au, biao.he.1990@gmail.com, hamidj@uci.edu

Abstract—We propose a novel analytical framework for evaluating the coverage performance of a millimeter wave (mmWave) cellular network where idle user equipments (UEs) act as relays. In this network, the base station (BS) adopts either the direct mode to transmit to the destination UE, or the relay mode if the direct mode fails, where the BS transmits to the relay UE and then the relay UE transmits to the destination UE. To address the drastic rotational movements of destination UEs in practice, we propose to adopt selection combining at destination UEs. New expression is derived for the signal-to-interference-plus-noise ratio (SINR) coverage probability of the network. Using numerical results, we first demonstrate the accuracy of our new expression. Then we show that ignoring spatial correlation, which has been commonly adopted in the literature, leads to severe overestimation of the SINR coverage probability. Furthermore, we show that introducing relays into a mmWave cellular network vastly improves the coverage performance. In addition, we show that the optimal BS density maximizing the SINR coverage probability can be determined by using our analysis.

I. INTRODUCTION

Millimeter wave (mmWave) has been widely acknowledged as a key enabler for multi-gigabit-per-second cellular networks [1], since the rich available spectrum at the mmWave band can effectively resolve the bandwidth shortage problem faced by global cellular operators. One of the most pressing challenges for mmWave cellular networks is to enhance the coverage performance, due to the unique properties of mmWave propagation such as its extreme sensitivity to blockage [2]. One promising strategy to enhance the coverage performance is to introduce relays into mmWave cellular networks for circumventing the blockage [3, 4]. The introduction of relays can be realized by either deploying infrastructure relays or allowing idle user equipments (UEs) to function as relays (e.g., idle UEs serve as device-to-device (D2D) transmitters) [4]. In this paper, we consider idle relay UEs since such relays have practical advantages relative to infrastructure relays, e.g., avoiding extra cost in infrastructure.

Motivated by the benefits of relays, the performance of relay assisted mmWave networks has been studied in the literature, e.g., [4–8]. For example, [5] investigated relay selection among multiple decode-and-forward (DF) relays between one base station (BS) and one UE. Focusing on an amplified-and-forward (AF) relay, [6] evaluated the maximum achievable rates for half-duplex and full-duplex relaying. It is noted that

neither [5] nor [6] considered multiple BSs or multiple UEs. To overcome such limitations, [7] investigated the coverage performance of a relay assisted mmWave cellular network with multiple BSs and multiple UEs while ignoring the interference in the network. Recently, [4] considered the interference when analyzing the coverage performance of a relay assisted mmWave cellular network. However, small scale fading was not considered in this analysis and directional combining was assumed at UEs.

The consideration of directional combining at multi-antenna UEs, such as [4], was commonly adopted in mmWave studies, e.g., [9–12]. The main rationale behind this consideration is that directional combining not only enhances the desired signal quality but also reduces the interference, under the assumption that the direction of the UE is perfectly aligned with its associated transmitter. However, as pointed out in [13], it is extremely difficult to keep this perfect alignment in practical usage scenarios, due to the frequent drastic rotational movements of UEs, especially when UEs are not idle. For example, when people play video games, the UE is frequently rotated since more and more video games need to exploit the gyroscopic sensor at the UE. Notably, the rotational movement when people play video games can be up to 80° per 100 ms [13]. When the UE adopts directional combining, its rotational movement causes a severe misalignment problem, which significantly damages the reliability of the mmWave cellular network [13]. Motivated by this, we propose to adopt *selection combining* at UEs when they receive downlink data. We emphasize that, unlike directional combining, selection combining does not incur misalignment problems since it does not require the UE to align its direction with its associated transmitter.

In this paper, we analyze the coverage performance of a relay assisted mmWave cellular network which consists of multiple BSs, multiple relay UEs, and multiple destination UEs. In this network, the BS transmits data either directly to the destination UE, or indirectly via the relay UE when the direct transmission fails. We propose a new analytical framework to derive the signal-to-interference-plus-noise ratio (SINR) coverage probability of the network. In this framework, we consider (1) generalized Nakagami- m fading, (2) interference, (3) selection combining at destination UEs, and

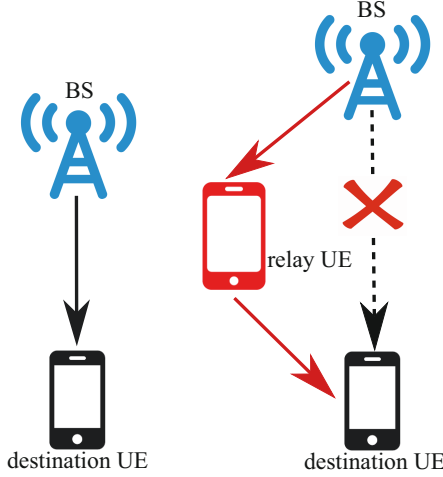


Fig. 1. The two transmission modes of the considered relay assisted mmWave cellular network.

(4) *spatial correlation*. Here, spatial correlation addresses the phenomenon that the received signals at the destination UE antennas are not independent, which has commonly been ignored in existing studies for simplifying analysis. Using numerical results, we first demonstrate the correctness of the derived SINR coverage probability. We also show that ignoring spatial correlation leads to severe overestimation of the coverage probability, as well as severe underestimation of the minimum number of antennas needed at destination UEs to achieve an SINR coverage probability target. We further show the benefit of introducing relays for coverage performance enhancement and that the optimal BS density maximizing the SINR coverage probability can be found through our analysis.

II. RELAY ASSISTED MMWAVE CELLULAR NETWORK

In this paper, we consider a relay assisted mmWave cellular network where BSs communicate with UEs. In this network, we assume that there are three types of UEs: 1) Destination UEs which are the UEs that require downlink data from BSs, 2) Uplink UEs which are the UEs that transmit uplink data to BSs, and 3) Relay UEs which are idle UEs that function as relays (or equivalently, D2D transmitters) to help the transmission between a BS and a destination UE. As depicted in Fig. 1, there are two transmission modes in the considered network: 1) Direct mode where the BS transmits data to the destination UE directly, and 2) Relay mode where the BS first transmits data to the relay UE and then the relay UE forwards data to the destination UE. Specifically, the relay mode serves as a backup option when the direct mode fails, i.e., the SINR of the direct link from the BS to the destination UE is below a given SINR threshold.

A. Locations of BSs and UEs

We assume that the locations of BSs, relay UEs, and destination UEs follow three PPPs in \mathbb{R}^2 , the densities of which are denoted by $\hat{\lambda}_b$, $\hat{\lambda}_r$, and $\hat{\lambda}_d$, respectively. In this paper, we randomly select one destination UE, refer to it as the typical destination UE, and establish a polar coordinate

system with the typical destination UE at the origin, \mathbf{o} . Based on the Slivnyak theorem, the conclusions drawn for the typical destination UE can be extended to other destination UEs.

We note that mmWave communications are extremely sensitive to blockage [2]. Moreover, the diffraction of mmWave propagation is weak due to the used high frequencies. Thus, in this work we only consider line-of-sight (LoS) links as in [11, 14]. To model the spatial distribution of LoS BSs and LoS relay UEs, we adopt an accurate and simple LoS ball model as in [11, 12, 15]. As per this model, the probability of a link being LoS, $P_{\text{LoS}}(\ell)$, is a function of the distance between the transmitter and the receiver, ℓ . Mathematically, $P_{\text{LoS}}(\ell)$ is given by

$$P_{\text{LoS}}(\ell) = \begin{cases} \varrho_\varepsilon, & \text{if } 0 < \ell < r_\varepsilon, \\ 0, & \text{otherwise,} \end{cases} \quad (1)$$

where $\varepsilon \in \{b, u\}$, r_b and r_u are the radii of the BS LoS ball and the relay UE LoS ball, respectively, and $0 \leq \varrho_b \leq 1$ and $0 \leq \varrho_u \leq 1$ are the LoS probabilities of BSs and relay UEs, respectively. According to the thinning theorem [16, Prop. (1.3.5)], the LoS BSs follow a PPP Φ_b with density $\lambda_b \triangleq \varrho_b \hat{\lambda}_b$ within the circular area $\mathcal{B}(\mathbf{o}, r_b)$. Similarly, the LoS relay UEs follow another PPP Φ_r with density $\lambda_r \triangleq \varrho_u \hat{\lambda}_r$ within the circular area $\mathcal{B}(\mathbf{o}, r_u)$. We denote the set of LoS BSs by $\Phi_b = \{b_0, b_1, b_2, \dots\}$, where b_0 is the associated BS, b_k is the k th interfering BS, and $k \in \{1, 2, \dots\}$.

B. Directional Gains

We assume that an N_b element uniform linear antenna array is adopted at each BS and an N_u element uniform linear antenna array is adopted at each UE. At BSs, highly directional beams are assumed to be adopted to combat the high path loss of mmWave transmission. Then we note that destination UEs often experience rapid rotational movements. Thus, we assume that the typical destination UE does not leverage directional beams to avoid the beam misalignment caused by rapid rotational movements. Instead, it adopts selection combining to choose the signal with the maximum SINR, out of N_u received SINRs at N_u antennas. Furthermore, we assume that relay UEs leverage directional beams since relay UEs are idle such that they do not experience rapid rotational movements.

To characterize the mmWave transmission in the network, we adopt the sectorized directional gain model [15, 17, 18] which incorporates key characteristics including the beamwidth, main lobe gain, and side lobe gain. Under the assumption that an N_b element uniform linear antenna array is adopted at each BS, the beamwidth, main lobe gain, and side lobe gain of BSs are given by $\theta_b = \frac{102\pi}{180N_b}$, $G_B = N_b$, and $G_b = \frac{1}{N_b}$, respectively. Similarly, the beamwidth, main lobe gain, and side lobe gain of relay UEs and uplink UEs are given by $\theta_u = \frac{102\pi}{180N_u}$, $G_U = N_u$, and $G_u = \frac{1}{N_u}$, respectively. Based on such notations, the directional gain of b_k , G_{b_k} , is a function of the angle off the boresight direction, θ_o , given by $G_{b_k} = G_B$, if $|\theta_o| \leq \frac{1}{2}\theta_b$, and $G_{b_k} = G_b$, otherwise. Here, we model θ_o as a uniform random variable between

$-\pi$ and π . Thus, G_{b_k} is a discrete random variable which equals G_B with probability (w. p.) $\frac{\theta_b}{2\pi}$, and G_b w. p. $1 - \frac{\theta_b}{2\pi}$. Similarly, the directional gain of relay UEs, G_e , is a discrete random variable which equals G_U w. p. $\frac{\theta_u}{2\pi}$, and G_u w. p. $1 - \frac{\theta_u}{2\pi}$. Furthermore, we define the directional gain from b_k to the relay UE as $G_{b_k r} \triangleq G_{b_k} G_e$. Thus, the probability mass function of $G_{b_k r}$ is given by

$$G_{b_k r} = \begin{cases} G_B G_U, & \text{w. p. } \frac{\theta_b \theta_u}{4\pi^2}, \\ G_B G_u, & \text{w. p. } \frac{\theta_b}{2\pi} \left(1 - \frac{\theta_u}{2\pi}\right), \\ G_b G_U, & \text{w. p. } \left(1 - \frac{\theta_b}{2\pi}\right) \frac{\theta_u}{2\pi}, \\ G_b G_u, & \text{w. p. } \left(1 - \frac{\theta_b}{2\pi}\right) \left(1 - \frac{\theta_u}{2\pi}\right). \end{cases} \quad (2)$$

C. Association Strategy

We assume that all BSs have the same transmit power, P_b , and all relay UEs and uplink UEs have the same transmit power, P_u . We then assume that the maximum signal strength association strategy is applied in the network. Thus, in the direct mode, the destination UE always associates with its nearest LoS BS, while in the relay mode, the destination UE always associates with its nearest LoS relay UE and the associated relay UE always associates with the associated relay UE's nearest LoS BS [4]. Thus, throughout this paper, the link from the associated BS to the typical destination UE is referred to as the *direct link*, the link from the associated BS to the associated relay UE is referred to as the *BR link*, and the link from the associated relay UE to the typical destination UE is referred to as the *RD link*. We denote the distances of the direct link, the BR link, and the RD link by ℓ_{bd} , ℓ_{br} , and ℓ_{rd} , respectively. If $\Phi_b \neq \emptyset$, the probability density function (PDF) of ℓ_{bd} is the same as the PDF of ℓ_{br} , which is given by $f_{\ell_{bd}}(x) = f_{\ell_{br}}(x) = 2\pi\lambda_b x e^{-\pi\lambda_b x^2} / \Xi_b$, where $\Xi_b \triangleq \Pr(\Phi_b \neq \emptyset) = 1 - e^{-\pi\lambda_b r_b^2}$ and $0 < x < r_b$ [16]. If $\Phi_r \neq \emptyset$, the PDF of ℓ_{rd} is given by $f_{\ell_{rd}}(x) = 2\pi\lambda_r x e^{-\pi\lambda_r x^2} / \Xi_r$, where $\Xi_r \triangleq \Pr(\Phi_r \neq \emptyset) = 1 - e^{-\pi\lambda_r r_u^2}$ and $0 < x < r_u$.

D. SINR Formulation

In this subsection, we first characterize the interference from the BS to the destination UE, the interference from the BS to the relay UE, and the interference from the relay UE to the destination UE. Then we formulate the SINRs between two nodes based on the interference characterization.

We assume that frequency division duplex is adopted, i.e., downlink frequency band and uplink frequency band are non-overlapping. Thus, the transmission using the downlink frequency band and the transmission using the uplink frequency band do not interfere with each other. In this network, we clarify that there are three types of transmitters: 1) BSs that transmit to destination UEs in the direct mode and relay UEs in the relay mode, 2) Relay UEs that transmit to destination UEs, and 3) Uplink UEs that transmit uplink data to BSs. Similar to [4], we assume that BSs transmit using the downlink frequency band, while relay UEs and uplink UEs transmit using the uplink frequency band. Thus, the transmission from BSs and the transmissions from relay UEs and uplink UEs do not interfere with each other, but the transmission from relay

UEs and the transmission from uplink UEs interfere with each other. It follows that in the direct link and the BR link, the interference solely comes from other BSs. Differently, in the RD link, the interference comes from not only other relay UEs but also uplink UEs.

We emphasize that not all relay UEs and uplink UEs interfere with the RD link. It is widely acknowledged that in a cellular network, network resources must be divided into multiple sub-channels to enable multiple access. In this paper, we assume that the UEs using the same sub-channel interfere with each other, while the UEs using different sub-channels do not. Thus, in the RD link, only the relay UEs and uplink UEs which use the same sub-channel as the associated relay UE cause interference. In the following, we define all interfering relay UEs and uplink UEs as interfering UEs. In order to model the distribution of all interfering UEs, we define a multiplexing factor, ρ , which represents the average number of interfering UEs on each sub-channel within the cell [4]. Considering the distribution of BSs, the distribution of LoS interfering UEs can be modeled by a homogeneous PPP with density $\lambda_i \triangleq \rho_u \rho \lambda_b$ within the circular area $\mathcal{B}(\mathbf{o}, r_u)$, $\Phi_i = \{i_1, i_2, \dots\}$, where i_k is the k th interfering UE and $k \in \{1, 2, \dots\}$.

Based on the aforementioned interference characterization, we obtain that the SINR at antenna n in the direct link, denoted by $\gamma_{bd,n}$ where $n \in \{1, 2, \dots, N_u\}$, is written as

$$\gamma_{bd,n} = \frac{P_b G_B \ell_{bd}^{-\eta} |h_{nb_0}|^2}{\sum_{b_k \in \tilde{\Phi}_b} P_b G_{b_k} \ell_{b_k d}^{-\eta} |h_{nb_k}|^2 + \sigma^2}, \quad (3)$$

where $\tilde{\Phi}_b \triangleq \Phi_b \setminus \{b_0\}$ denotes the set of LoS BSs excluding b_0 , $\ell_{b_k d}$ is the distance between b_k and the typical destination UE, $\eta \geq 2$ is the path loss exponent, h_{nb_l} is the small scale fading from b_l to antenna n , $l \in \{0, k\}$, and σ^2 is the variance of the additive white Gaussian noise (AWGN) at antenna n . In this work, we assume that h_{nb_l} is subject to independent and identically distributed (i.i.d.) Nakagami- m fading¹. By defining $\tilde{h}_{nb_l} \triangleq |h_{nb_l}|^2$, we find that \tilde{h}_{nb_l} follows the Gamma distribution with the shape parameter m_{bd} and the scale parameter $\frac{1}{m_{bd}}$, i.e., $\tilde{h}_{nb_l} \sim \Gamma\left(m_{bd}, \frac{1}{m_{bd}}\right)$.

In the BR link, the SINR at the relay UE, denoted by γ_{br} , is written as

$$\gamma_{br} = \frac{P_b G_B G_U \ell_{br}^{-\eta} \tilde{h}_{b_0}}{\sum_{b_k \in \tilde{\Phi}_b} P_b G_{b_k r} \ell_{b_k r}^{-\eta} \tilde{h}_{b_k} + \sigma^2}, \quad (4)$$

where $\ell_{b_k r}$ is the distance between b_k and the relay UE, \tilde{h}_{b_l} is the small scale fading gain between b_l and the relay UE, $l \in \{0, k\}$. In this work, we assume that \tilde{h}_{b_l} is subject to i.i.d. Gamma distribution with the shape parameter m_{br} and the scale parameter $\frac{1}{m_{br}}$, i.e., $\tilde{h}_{b_l} \sim \Gamma\left(m_{br}, \frac{1}{m_{br}}\right)$.

In the RD link, the SINR at antenna n , $n \in \{1, 2, \dots, N_u\}$,

¹We clarify that Nakagami- m fading is a generalized fading model which can fit a variety of empirical measurements, such as Rayleigh fading by setting $m = 1$ and Rician- K fading by setting $m = (K + 1)^2 / (2K + 1)$.

denoted by $\gamma_{rd,n}$, is written as

$$\gamma_{rd,n} = \frac{P_u G_U \ell_{rd}^{-\eta} \tilde{h}_{nr}}{\sum_{i_k \in \Phi_i} P_u G_e \ell_{ikd}^{-\eta} \tilde{h}_{ni_k} + \sigma^2}, \quad (5)$$

where ℓ_{ikd} is the distance between the k th interfering UE and the destination UE, \tilde{h}_{nr} is the small scale fading gain from the relay UE to antenna n , \tilde{h}_{ni_k} is the small scale fading from i_k to antenna n . In this work, we assume that \tilde{h}_{nr} and \tilde{h}_{ni_k} are subject to i.i.d. Gamma distribution with the shape parameter m_{rd} and the scale parameter $\frac{1}{m_{rd}}$, i.e., $\tilde{h}_{nr} \sim \Gamma\left(m_{rd}, \frac{1}{m_{rd}}\right)$ and $\tilde{h}_{ni_k} \sim \Gamma\left(m_{rd}, \frac{1}{m_{rd}}\right)$.

Under the assumption that the Nakagami- m fading parameters, e.g., m_{bd} , m_{br} , and m_{rd} , are positive integers [11, 17], the moment generating function (MGF) of \tilde{h}_μ is given by $M_{\tilde{h}_\mu}(s) = \left(1 - \frac{s}{m_\nu}\right)^{-m_\nu}$, where $(\mu, \nu) \in \{(nb_l, m_{bd}), (b_l, m_{br}), (nr, m_{rd}), (ni_k, m_{rd})\}$. Moreover, as given in [19, Lemma 1], the cumulative distribution function (CDF) of \tilde{h}_μ can be tightly lower bounded by

$$F_{\tilde{h}_\mu}(x) = 1 - e^{-m_\nu x} \sum_{\omega=0}^{m_\nu-1} \frac{(m_\nu x)^\omega}{\omega!} > (1 - e^{-\alpha_\nu x})^{m_\nu}, \quad (6)$$

where $\alpha_\nu = m_\nu (m_\nu!)^{-\frac{1}{m_\nu}}$. In the analysis presented in Section III, we adopt the lower bound on $F_{\tilde{h}_\mu}(x)$ since this lower bound enables us to derive the SINR coverage probability when the Nakagami- m fading parameters are higher than one.

By observing (3) and (5), we find that the interference signals at the N_u UE antennas are correlated due to the common interfering BSs' location or the common interfering UEs' location. Also, the desired signals at the N_u UE antennas are correlated due to the common associated BS' location or the common associated relay UE's location. Despite that both interference signals and desired signals are correlated in wireless networks, these spatial correlations are often ignored in the existing studies on mmWave systems to simplify the analysis. To overcome this, we address the spatial correlation when analyzing the coverage performance of the network considered in this paper.

III. SINR COVERAGE PROBABILITY ANALYSIS

In this section, we derive the SINR coverage probability of the considered network, $\mathbb{P}_{N_u}(\tau)$. Here, $\mathbb{P}_{N_u}(\tau)$ is defined as the probability that the SINR at the N_u -antenna typical destination UE is higher than a given SINR threshold, τ . As aforementioned, we derive $\mathbb{P}_{N_u}(\tau)$ by considering spatial correlation at the destination UE. This mandates a new and challenging analytical framework for the SINR coverage probability, as pointed out in [20]. Furthermore, we aim to answer an open question in mmWave cellular networks: “*Is the analysis error caused by ignoring spatial correlation acceptable?*” To answer this question, we also derive the SINR coverage probability for the case where spatial correlation is ignored, which enables us to compare the two coverage probabilities in Section IV.

We assume that the half-duplex DF relay protocol is adopted. Thus, in the relay mode, the SINR at the typical destination UE is higher than τ when both the SINR of the BR link and the SINR of the RD link are higher than τ . We denote the SINR coverage probability of the direct link, the BR link, and the RD link as $\mathbb{P}_{N_u,bd}(\tau)$, $\mathbb{P}_{br}(\tau)$, and $\mathbb{P}_{N_u,rd}(\tau)$, respectively. This allows us to express $\mathbb{P}_{N_u}(\tau)$ as

$$\mathbb{P}_{N_u}(\tau) = 1 - [1 - \mathbb{P}_{N_u,bd}(\tau)][1 - \mathbb{P}_{br}(\tau)\mathbb{P}_{N_u,rd}(\tau)]. \quad (7)$$

We next derive and present $\mathbb{P}_{N_u,bd}(\tau)$, $\mathbb{P}_{br}(\tau)$, and $\mathbb{P}_{N_u,rd}(\tau)$ in Theorems 1, 2, and 3, respectively.

Theorem 1: Under the assumption that $F_{\tilde{h}_{nb_l}}(x)$ is approximated as $(1 - e^{-\alpha_{bd}x})^{m_{bd}}$, the SINR coverage probability of the direct link is derived as

$$\begin{aligned} \mathbb{P}_{N_u,bd}(\tau) &= \Xi_b \sum_{\kappa=1}^{N_u} (-1)^{\kappa+1} \binom{N_u}{\kappa} \sum_{j_1+j_2+\dots+j_{m_{bd}}=\kappa} \beta_{bd} \\ &\times \int_0^{\tau b} e^{-\frac{\tau \alpha_{bd} \Omega_{bd} \sigma^2}{P_b G_B x^{-\eta}} - 2\pi \lambda_b \int_x^{\tau b} \ell(1-v_{bd}(\ell))d\ell} f_{\ell_{bd}}(x) dx, \end{aligned} \quad (8)$$

where $j_1, j_2, \dots, j_{m_{bd}}$ are nonnegative integers, $\Omega_{bd} \triangleq j_1 + 2j_2 + \dots + m_{bd}j_{m_{bd}}$, $\delta_{bd} \triangleq \frac{\alpha_{bd}\tau}{P_b G_B \ell_{bd}^{-\eta}}$, β_{bd} is defined as

$$\begin{aligned} \beta_{bd} &\triangleq \binom{\kappa}{j_1} \binom{\kappa-j_1}{j_2} \dots \binom{\kappa-j_1-\dots-j_{m_{bd}-1}}{j_{m_{bd}}} \binom{m_{bd}}{1}^{j_1} \\ &\times \binom{m_{bd}}{2}^{j_2} \dots \binom{m_{bd}}{m_{bd}}^{j_{m_{bd}}} (-1)^{j_1+j_2+\dots+j_{m_{bd}}+\Omega_{bd}}, \end{aligned} \quad (9)$$

and $v_{bd}(\ell)$ is defined as

$$\begin{aligned} v_{bd}(\ell) &\triangleq \frac{\theta_b}{2\pi} \prod_{q=1}^{m_{bd}} \left(1 + \frac{q\delta_{bd}P_b G_B \ell^{-\eta}}{m_{bd}}\right)^{-m_{bd}j_q} \\ &+ \left(1 - \frac{\theta_b}{2\pi}\right) \prod_{q=1}^{m_{bd}} \left(1 + \frac{q\delta_{bd}P_b G_b \ell^{-\eta}}{m_{bd}}\right)^{-m_{bd}j_q}. \end{aligned} \quad (10)$$

Proof: We define ϵ_n as the event that $\gamma_{bd,n}$ is higher than τ , where $n \in \{1, 2, \dots, N_u\}$. As per the rules of selection combining, $\mathbb{P}_{N_u,bd}(\tau)$ is written as

$$\begin{aligned} \mathbb{P}_{N_u,bd}(\tau) &= \Pr\left(\bigcup_{n=1}^{N_u} \epsilon_n\right) \\ &= \sum_{\kappa=1}^{N_u} (-1)^{\kappa+1} \sum_{1 \leq \zeta_1 < \zeta_2 < \dots < \zeta_\kappa \leq N_u} \Pr(\epsilon_{\zeta_1} \cap \epsilon_{\zeta_2} \cap \dots \cap \epsilon_{\zeta_\kappa}). \end{aligned} \quad (11)$$

We note that in the considered network, the probability of the intersection of κ events, $\Pr(\epsilon_{\zeta_1} \cap \epsilon_{\zeta_2} \cap \dots \cap \epsilon_{\zeta_\kappa})$, is the same, regardless of which κ out of N_u events are chosen. Thus, we rewrite (11) as

$$\mathbb{P}_{N_u,bd}(\tau) = \sum_{\kappa=1}^{N_u} (-1)^{\kappa+1} \binom{N_u}{\kappa} \Pr\left(\bigcap_{n=1}^{\kappa} \epsilon_n\right). \quad (12)$$

Based on (3), we derive $\Pr\left(\bigcap_{n=1}^{\kappa} \epsilon_n\right)$ as

$$\begin{aligned} & \Pr\left(\bigcap_{n=1}^{\kappa} \epsilon_n\right) \\ &= \Xi_b \Pr\left(\bigcap_{n=1}^{\kappa} \tilde{h}_{nb_0} > \frac{\tau \left(\sum_{b_k \in \tilde{\Phi}_b} P_b G_{b_k} \ell_{b_k d}^{-\eta} \tilde{h}_{nb_k} + \sigma^2\right)}{P_b G_B \ell_{bd}^{-\eta}}\right) \\ &\stackrel{(f)}{=} \Xi_b \mathbb{E}_{\ell_{bd}, \tilde{\Phi}_b, G_{b_k}, \vartheta} \left[\prod_{n=1}^{\kappa} \sum_{j=1}^{m_{bd}} \binom{m_{bd}}{j} (-1)^{j+1} \right. \\ &\quad \left. \times e^{-j\delta_{bd} \left(\sum_{b_k \in \tilde{\Phi}_b} P_b G_{b_k} \ell_{b_k d}^{-\eta} \tilde{h}_{nb_k} + \sigma^2\right)} \right]. \end{aligned} \quad (13)$$

Here, step (f) is achieved by following the binomial theorem and making the assumption that $F_{\tilde{h}_{nb_l}}(x)$ is approximated as $(1 - e^{-\alpha_{bd}x})^{m_{bd}}$, while ϑ is defined as $\vartheta \triangleq \sum_{q=1}^{m_{bd}} \sum_{p=1}^{j_q} q \tilde{h}_{I_{q,p}, b_k}$, where $I_{q,p} \in \{1, \dots, \kappa\}$ with $q \in \{1, \dots, m_{bd}\}$ and $p \in \{1, \dots, j_q\}$ and the values of $I_{q,p}$ differ from each other. By defining $\Psi = \sum_{b_k \in \tilde{\Phi}_b} \delta_{bd} P_b G_{b_k} \ell_{b_k d}^{-\eta} \vartheta$, we further derive (13) as

$$\begin{aligned} & \Pr\left(\bigcap_{n=1}^{\kappa} \epsilon_n\right) \\ &= \Xi_b \sum_{j_1+j_2+\dots+j_{m_{bd}}=\kappa} \mathbb{E}_{\ell_{bd}} \left[e^{-\delta_{bd} \sigma^2 \Omega_{bd}} \sum_{I_{q,p}} \mathbb{E}_{\tilde{\Phi}_b, G_{b_k}, \vartheta} \left[e^{-\Psi} \right] \right] \\ &\quad \times \binom{m_{bd}}{1}^{j_1} \binom{m_{bd}}{2}^{j_2} \dots \binom{m_{bd}}{m_{bd}}^{j_{m_{bd}}} (-1)^{j_1+j_2+\dots+j_{m_{bd}}+\Omega_{bd}} \\ &\stackrel{(g)}{=} \Xi_b \sum_{j_1+j_2+\dots+j_{m_{bd}}=\kappa} \beta_{bd} \mathbb{E}_{\ell_{bd}} \left[e^{-\delta_{bd} \sigma^2 \Omega_{bd}} \mathbb{E}_{\tilde{\Phi}_b, G_{b_k}, \vartheta} \left[e^{-\Psi} \right] \right]. \end{aligned} \quad (14)$$

To achieve step (g), we find that given $M_{\tilde{h}_{nb_l}}(s)$, the MGF of ϑ is $M_{\vartheta}(s) = \prod_{q=1}^{m_{bd}} \left(1 - \frac{qs}{m_{bd}}\right)^{-m_{bd}j_q}$. This indicates that given $j_1, j_2, \dots, j_{m_{bd}}$, the MGF of ϑ does not change with the values of $I_{q,p}$. We also find that given $j_1, j_2, \dots, j_{m_{bd}}$, $\mathbb{E}_{\tilde{\Phi}_b, G_{b_k}, \vartheta} [e^{-\Psi}]$ does not change with the values of $I_{q,p}$. Thus, step (g) is achieved due to $\sum_{I_{q,p}} \mathbb{E}_{\tilde{\Phi}_b, G_{b_k}, \vartheta} [e^{-\Psi}] = \binom{k}{j_1} \binom{k-j_1}{j_2} \dots \binom{k-j_1-\dots-j_{m_{bd}-1}}{j_{m_{bd}}} \mathbb{E}_{\tilde{\Phi}_b, G_{b_k}, \vartheta} [e^{-\Psi}]$.

Using the MGF of ϑ , we derive $\mathbb{E}_{\tilde{\Phi}_b, G_{b_k}, \vartheta} [e^{-\Psi}]$ as

$$\begin{aligned} & \mathbb{E}_{\tilde{\Phi}_b, G_{b_k}, \vartheta} [e^{-\Psi}] \\ &= \mathbb{E}_{\tilde{\Phi}_b, G_{b_k}, \vartheta} \left[\prod_{\tilde{\Phi}_b} e^{-\delta_{bd} P_b G_{b_k} \ell_{b_k d}^{-\eta} \vartheta} \right] \\ &\stackrel{(h)}{=} \mathbb{E}_{\tilde{\Phi}_b, G_{b_k}} \left[\prod_{\tilde{\Phi}_b} \prod_{q=1}^{m_{bd}} \left(1 + \frac{q \delta_{bd} P_b G_{b_k} \ell_{b_k d}^{-\eta}}{m_{bd}}\right)^{-m_{bd}j_q} \right] \\ &= \mathbb{E}_{\tilde{\Phi}_b} \left[\prod_{\tilde{\Phi}_b} v_{bd}(\ell_{b_k d}) \right] \\ &= e^{-2\pi\lambda_b \int_{\ell_{bd}}^{r_b} \ell(1-v_{bd}(\ell))d\ell}. \end{aligned} \quad (15)$$

Here, step (h) is achieved by using $M_{\vartheta}(s)$. Finally, by substituting (14) and (15) into (12), we obtain the desired result in (8) and complete the proof. ■

Theorem 2: Under the assumption that the CDF of \tilde{h}_{b_l} is approximated as $(1 - e^{-\alpha_{br}x})^{m_{br}}$, the SINR coverage probability of the BR link is derived as

$$\begin{aligned} \mathbb{P}_{br}(\tau) &= \Xi_b \sum_{j=1}^{m_{br}} (-1)^{j+1} \binom{m_{br}}{j} \\ &\quad \times \int_0^{r_b} e^{-\psi x^{\eta} \sigma^2 - 2\pi\lambda_b \int_x^{r_b} \ell \Omega_b d\ell} f_{\ell_{br}}(x) dx, \end{aligned} \quad (16)$$

where $\psi \triangleq \frac{j\alpha_{br}\tau}{P_b G_B G_U}$ and Ω_b is defined as (17).

Proof: Based on (4), we derive $\mathbb{P}_{br}(\tau)$ as

$$\begin{aligned} & \mathbb{P}_{br}(\tau) \\ &= \Xi_b \mathbb{E}_{\ell_{br}, I_b^*} \left[\Pr\left(\tilde{h}_{b_0} > \frac{\tau(I_b^* + \sigma^2)}{P_b G_B G_U \ell_{br}^{-\eta}}\right) \right] \\ &\stackrel{(i)}{=} \Xi_b \mathbb{E}_{\ell_{br}, I_b^*} \left[\sum_{j=1}^{m_{br}} (-1)^{j+1} \binom{m_{br}}{j} e^{-\frac{j\alpha_{br}\tau(I_b^* + \sigma^2)}{P_b G_B G_U \ell_{br}^{-\eta}}} \right] \\ &= \Xi_b \sum_{j=1}^{m_{br}} (-1)^{j+1} \binom{m_{br}}{j} \mathbb{E}_{\ell_{br}, I_b^*} \left[e^{-\frac{\psi(I_b^* + \sigma^2)}{\ell_{br}^{-\eta}}} \right] \\ &= \Xi_b \sum_{j=1}^{m_{br}} (-1)^{j+1} \binom{m_{br}}{j} \mathbb{E}_{\ell_{br}} \left[e^{-\frac{\psi\sigma^2}{\ell_{br}^{-\eta}}} \mathbb{E}_{I_b^*} \left[e^{-\frac{\psi I_b^*}{\ell_{br}^{-\eta}}} \right] \right] \\ &= \Xi_b \sum_{j=1}^{m_{br}} (-1)^{j+1} \binom{m_{br}}{j} \\ &\quad \times \int_0^{r_b} e^{-\psi x^{\eta} \sigma^2} \mathbb{E}_{I_b^*} \left[e^{-\frac{\psi I_b^*}{x^{-\eta}}} \right] f_{\ell_{br}}(x) dx, \end{aligned} \quad (18)$$

where $I_b^* \triangleq \sum_{b_k \in \tilde{\Phi}_b} P_b G_{b_k r} \ell_{b_k r}^{-\eta} \tilde{h}_{b_k}$. Here, step (i) is achieved by following the binomial theorem and making the assumption that the CDF of \tilde{h}_{b_l} is approximated as $(1 - e^{-\alpha_{br}x})^{m_{br}}$. We further derive $\mathbb{E}_{I_b^*} \left[e^{-\frac{\psi I_b^*}{x^{-\eta}}} \right]$ as

$$\begin{aligned} & \mathbb{E}_{I_b^*} \left[e^{-\frac{\psi I_b^*}{x^{-\eta}}} \right] = \mathbb{E}_{I_b^*} \left[e^{-\psi x^{\eta} I_b^*} \right] \\ &\stackrel{(j)}{=} e^{-\lambda_b \int_x^{r_b} \ell \int_0^{2\pi} \left(1 - \mathbb{E}_{\tilde{h}_{b_k}} \left[e^{-\tilde{h}_{b_k} \psi x^{\eta} P_b G_{b_k r} \ell^{-\eta}} \right] \right) d\theta d\ell} \\ &\stackrel{(k)}{=} e^{-\lambda_b \int_x^{r_b} \ell \int_0^{2\pi} \left(1 - \left(1 + \frac{\psi x^{\eta} P_b G_{b_k r} \ell^{-\eta}}{m_{br}}\right)^{-m_{br}}\right) d\theta d\ell} \\ &\stackrel{(l)}{=} e^{-2\pi\lambda_b \int_x^{r_b} \ell \Omega_b d\ell}. \end{aligned} \quad (19)$$

Here, step (j) is achieved as per [16, Cor. (2.3.2)], step (k) is achieved by using the MGF of Gamma distribution, and step (l) is achieved as per (2). Finally, we substitute (19) into (18) to obtain the desired result in (16) and thus, the proof is completed. ■

Theorem 3: Under the assumption that the CDFs of \tilde{h}_{nr} and \tilde{h}_{ni_k} are approximated as $(1 - e^{-\alpha_{rd}x})^{m_{rd}}$, the SINR

$$\Omega_b \triangleq \frac{\theta_u}{2\pi} \left(1 - \frac{\theta_b}{2\pi}\right) \left[1 - \left(1 + \frac{\psi x^\eta P_b G_b G_U}{m_{br} \ell^\eta}\right)^{-m_{br}}\right] + \left(1 - \frac{\theta_b}{2\pi}\right) \left(1 - \frac{\theta_u}{2\pi}\right) \left[1 - \left(1 + \frac{\psi x^\eta P_b G_b G_u}{m_{br} \ell^\eta}\right)^{-m_{br}}\right] \\ + \frac{\theta_b}{2\pi} \left(1 - \frac{\theta_u}{2\pi}\right) \left[1 - \left(1 + \frac{\psi x^\eta P_b G_B G_u}{m_{br} \ell^\eta}\right)^{-m_{br}}\right] + \frac{\theta_b}{2\pi} \frac{\theta_u}{2\pi} \left[1 - \left(1 + \frac{\psi x^\eta P_b G_B G_U}{m_{br} \ell^\eta}\right)^{-m_{br}}\right]. \quad (17)$$

coverage probability of the RD link is derived as

$$\mathbb{P}_{N_u,rd}(\tau) = \Xi_r \sum_{\kappa=1}^{N_u} (-1)^{\kappa+1} \binom{N_u}{\kappa} \sum_{j_1+j_2+\dots+j_{m_{rd}}=\kappa} \beta_{rd} \\ \times \int_0^{r_u} e^{-\frac{\tau \alpha_{rd} \Omega_{rd} \sigma^2}{P_u G_U x^{-\eta}} - 2\pi \lambda_i \int_0^{r_u} \ell(1-v_{rd}(\ell)) d\ell} f_{\ell_{rd}}(x) dx, \quad (20)$$

where $j_1, j_2, \dots, j_{m_{rd}}$ are nonnegative integers, $\Omega_{rd} \triangleq j_1 + 2j_2 + \dots + m_{rd}j_{m_{rd}}$, $\delta_{rd} \triangleq \frac{\alpha_{rd}\tau}{P_u G_U \ell_{rd}^{-\eta}}$, β_{rd} is defined as

$$\beta_{rd} \triangleq \binom{\kappa}{j_1} \binom{\kappa-j_1}{j_2} \dots \binom{\kappa-j_1-\dots-j_{m_{rd}-1}}{j_{m_{rd}}} \binom{m_{rd}}{1}^{j_1} \\ \times \binom{m_{rd}}{2}^{j_2} \dots \binom{m_{rd}}{m_{rd}}^{j_{m_{rd}}} (-1)^{j_1+j_2+\dots+j_{m_{rd}}+\Omega_{rd}}, \quad (21)$$

and $v_{rd}(\ell)$ is defined as

$$v_{rd}(\ell) \triangleq \frac{\theta_u}{2\pi} \prod_{q=1}^{m_{rd}} \left(1 + \frac{q\delta_{rd} P_u G_U \ell^{-\eta}}{m_{rd}}\right)^{-m_{rd}j_q} \\ + \left(1 - \frac{\theta_u}{2\pi}\right) \prod_{q=1}^{m_{rd}} \left(1 + \frac{q\delta_{rd} P_u G_u \ell^{-\eta}}{m_{rd}}\right)^{-m_{rd}j_q}. \quad (22)$$

Proof: The proof of Theorem 3 is omitted here because (20) can be obtained by following the procedure presented in the proof of Theorem 1. ■

We now examine the case where spatial correlation is ignored. In this case, the SINRs received at the N_u antennas of the destination UE are assumed to be independent with each other. Thus, when spatial correlation is ignored, the SINR coverage probability of the direct link, $\hat{\mathbb{P}}_{N_u,bd}(\tau)$, is given by

$$\hat{\mathbb{P}}_{N_u,bd}(\tau) = 1 - (1 - \mathbb{P}_{1,bd}(\tau))^{N_u}, \quad (23)$$

and the SINR coverage probability of the RD link, $\hat{\mathbb{P}}_{N_u,rd}(\tau)$, is given by

$$\hat{\mathbb{P}}_{N_u,rd}(\tau) = 1 - (1 - \mathbb{P}_{1,rd}(\tau))^{N_u}. \quad (24)$$

Therefore, when spatial correlation is ignored, the probability that the SINR at the N_u -antenna typical destination UE is higher than τ , $\hat{\mathbb{P}}_{N_u}(\tau)$, is obtained as

$$\hat{\mathbb{P}}_{N_u}(\tau) = 1 - \left[1 - \hat{\mathbb{P}}_{N_u,bd}(\tau)\right] \left[1 - \mathbb{P}_{br}(\tau) \hat{\mathbb{P}}_{N_u,rd}(\tau)\right]. \quad (25)$$

The difference between (7) and (25) indicates that spatial correlation imposes a profound impact on the SINR coverage probability of the N_u -antenna destination UE. This will be further examined in Section IV.

TABLE I
SIMULATION PARAMETERS USED IN SECTION IV

Parameter	Value
BS transmit power, P_b	35 dBm
UE transmit power, P_u	25 dBm
Noise power, σ^2	0 dBm
Number of antennas at each BS, N_b	10
Number of antennas at each UE, N_u	4
Path loss exponent, η	2.4
Nakagami- m fading parameters, m_{bd}, m_{br}, m_{rd}	2
BS LoS ball radius, r_b	100 m
UE LoS ball radius, r_u	20 m
BS LoS probability, ϱ_b	0.9
UE LoS probability, ϱ_u	0.63
LoS BS density, λ_b	0.0002/m ²
LoS relay UE density, λ_r	0.002/m ²
Multiplexing factor, ρ	0.9

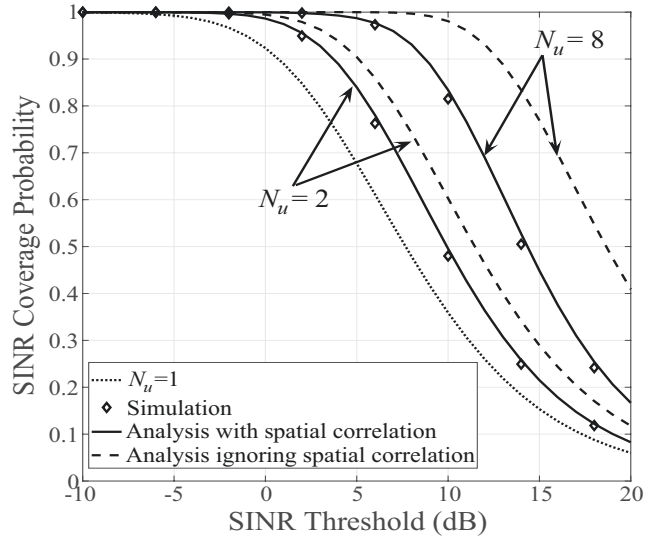


Fig. 2. The SINR coverage probability, $\mathbb{P}_{N_u}(\tau)$, versus the SINR threshold, τ , for different values of N_u .

IV. NUMERICAL RESULTS

In this section, we present numerical results to evaluate the impact of spatial correlation and network parameters on the SINR coverage probability, $\mathbb{P}_{N_u}(\tau)$. The values of the parameters used in this section are summarized in Table I, unless otherwise specified.

First, we examine the impact of spatial correlation and N_u on $\mathbb{P}_{N_u}(\tau)$ in Fig. 2. We observe that our analysis with spatial correlation given by (7) matches the simulations very well, which confirms that (7) is an accurate approximation. Moreover, we observe that $\mathbb{P}_{N_u}(\tau)$ significantly increases when N_u

TABLE II
 N_{\min} VERSUS \hat{N}_{\min} FOR DIFFERENT VALUES OF ξ

ξ	60%	70%	80%	90%
N_{\min}	4	5	7	12
\hat{N}_{\min}	2	3	4	5

increases. Specifically, when $\tau = 10$ dB, $\mathbb{P}_{N_u}(\tau)$ increases from 0.36 to 0.48 and then to 0.82 when N_u increases from 1 to 2 and then to 8. Furthermore, we observe that ignoring spatial correlation leads to severe overestimation of the SINR coverage probability, which is evident when comparing the analysis ignoring spatial correlation, given by (25), with Monte Carlo simulation points. Specifically, when $\tau = 14$ dB and $N_u = 8$, $\hat{\mathbb{P}}_{N_u}(\tau)$ is 0.83 while the simulation shows that the actual SINR coverage probability is 0.51. Indeed, spatial correlation significantly reduces the probability of successful reception at the destination UE, thus cannot be ignored.

In order to further examine the analysis error caused by ignoring spatial correlation, we investigate the minimum number of antennas needed at the destination UE to achieve a given SINR coverage probability target, ξ , for a given τ . Mathematically, it is expressed as $N_{\min} \triangleq \min \{N_u : \mathbb{P}_{N_u}(\tau) > \xi\}$ when spatial correlation is considered. When spatial correlation is ignored, the expression is $\hat{N}_{\min} \triangleq \min \{N_u : \hat{\mathbb{P}}_{N_u}(\tau) > \xi\}$. Table II shows N_{\min} and \hat{N}_{\min} for different ξ when $\tau = 10$ dB. This table confirms the underestimation of the minimum number of antennas needed when spatial correlation is ignored. For example, when $\xi = 90\%$, if spatial correlation is ignored, the minimum number of antennas needed is 5. However, the actual minimum number of antennas needed is 12. Again, this example shows that ignoring spatial correlation is not acceptable when designing relay assisted mmWave cellular networks.

We now examine the impact of the transmit power at the BS, P_b , on $\mathbb{P}_{N_u}(\tau)$ and compare the SINR coverage probability without relays with $\mathbb{P}_{N_u}(\tau)$ in Fig. 3. We remark that the SINR coverage probability without relays is $\mathbb{P}_{N_u,bd}(\tau)$, since without relays, the relay mode does not exist. We observe that $\mathbb{P}_{N_u}(\tau)$ increases as P_b increases. This is due to the fact that both $\gamma_{bd,n}$ and γ_{br} increase as P_b increases. Moreover, we observe that $\mathbb{P}_{N_u}(\tau)$ is significantly higher than $\mathbb{P}_{N_u,bd}(\tau)$. Specifically, when $\tau = 10$ dB, $N_u = 8$, and $P_b = 35$ dBm, $\mathbb{P}_{N_u}(\tau)$ is 0.83 while $\mathbb{P}_{N_u,bd}(\tau)$ is 0.59. This confirms that introducing relays into a mmWave cellular network vastly improves the SINR coverage probability. Furthermore, we observe that the gain brought by relays, i.e., the gap between $\mathbb{P}_{N_u}(\tau)$ and $\mathbb{P}_{N_u,bd}(\tau)$, becomes larger when N_u increases from 2 to 8, especially when P_b is not high, e.g., $P_b = 30 - 40$ dBm. This is due to the fact that when N_u increases, the directional gain of relay UEs, given by $G_U = N_u$, increases. When G_U increases, γ_{br} and $\gamma_{rd,n}$ increase. Thus, $\mathbb{P}_{br}(\tau)$ and $\mathbb{P}_{N_u,rd}(\tau)$ increase as N_u increases. Hence, based on (7), the gain brought by relays increases as N_u increases.

Finally, we examine the impact of the LoS BS density, λ_b ,

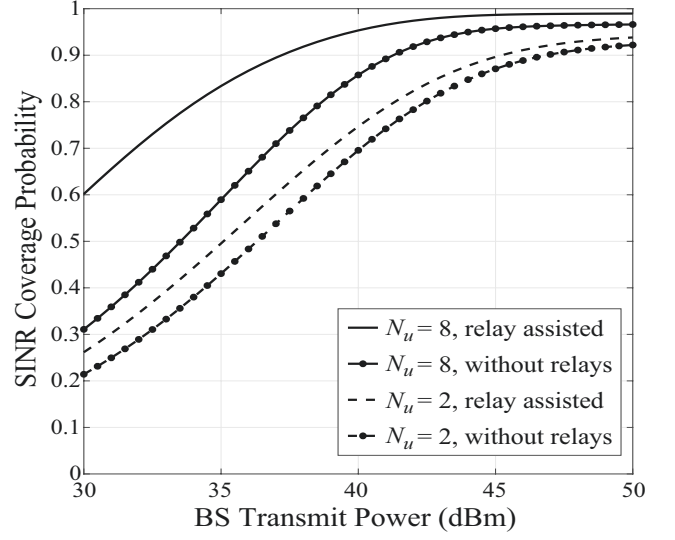


Fig. 3. The SINR coverage probability, $\mathbb{P}_{N_u}(\tau)$, versus the BS transmit power, P_b , for different values of N_u , with $\tau = 10$ dB.

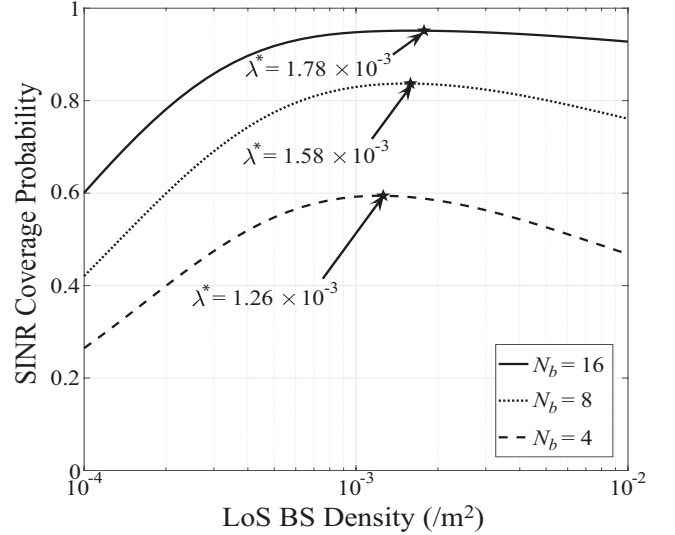


Fig. 4. The SINR coverage probability, $\mathbb{P}_{N_u}(\tau)$, versus the LoS BS density, λ_b , for different values of N_b , with $\tau = 10$ dB.

and the number of antennas at the BS, N_b , on $\mathbb{P}_{N_u}(\tau)$ in Fig. 4. We observe that $\mathbb{P}_{N_u}(\tau)$ first increases then decreases as λ_b increases. This is due to the fact that the impact of deploying more BSs is twofold. First, the associated BS is closer, which increases the desired signal power. Second, there are more interfering BSs, which increases the interference power. When λ_b increases from $10^{-4}/\text{m}^2$, the first impact dominates the second. After λ_b exceeds a certain value, which is the optimal BS density, λ_b^* , the second impact dominates the first. Thus, we highlight that λ_b^* that maximizes $\mathbb{P}_{N_u}(\tau)$ can be numerically found with the aid of our analysis. Specifically, when $N_b = 4, 8$, and 16 , the optimal BS densities are $\lambda_b^* = 1.26 \times 10^{-3}/\text{m}^2$, $1.58 \times 10^{-3}/\text{m}^2$, and $1.78 \times 10^{-3}/\text{m}^2$,

respectively. In addition, we observe that $\mathbb{P}_{N_u}(\tau)$ increases as N_b increases. Specifically, when $\lambda_b = 10^{-3}/\text{m}^2$, $\mathbb{P}_{N_u}(\tau)$ increases from 0.59 to 0.83 and then to 0.95 when N_b increases from 4 to 8 and then to 16. This observation is expected because the BS beamwidth, given by $\theta_b = \frac{102\pi}{180N_b}$, decreases as N_b increases and BSs with narrower beams cause less interference.

V. CONCLUSION

In this paper, we proposed a new analytical framework for the relay assisted mmWave cellular network which adopts selection combining at destination UEs to avoid the misalignment problem caused by traditional directional combining. Our results showed that ignoring spatial correlation to simplify the analysis is unacceptable, since it leads to severe over-estimation of the SINR coverage probability. Moreover, our results showed that introducing relays into a mmWave cellular network vastly improves the SINR coverage performance. Furthermore, we examined the impact of network parameters such as the BS density on the SINR coverage probability and found that the optimal BS density which maximizes the SINR coverage probability can be determined by using our analysis.

ACKNOWLEDGMENT

This work was funded by the Australian Research Council Discovery Project DP180104062 and the NSF Award ECCS-1642536.

REFERENCES

- [1] S. Rangan, T. S. Rappaport, and E. Erkip, "Millimeter-wave cellular wireless networks: Potentials and challenges," *Proc. IEEE*, vol. 102, no. 3, pp. 366–385, Mar. 2014.
- [2] Z. Pi and F. Khan, "An introduction to millimeter-wave mobile broadband systems," *IEEE Commun. Mag.*, vol. 49, no. 6, pp. 101–107, June 2011.
- [3] N. Wei, X. Lin, and Z. Zhang, "Optimal relay probing in millimeter-wave cellular systems with device-to-device relaying," *IEEE Trans. Veh. Technol.*, vol. 65, no. 12, pp. 10 218–10 222, Dec. 2016.
- [4] S. Wu, R. Atat, N. Mastronarde, and L. Liu, "Improving the coverage and spectral efficiency of millimeter-wave cellular networks using device-to-device relays," *IEEE Trans. Commun.*, vol. 66, no. 5, pp. 2251–2265, May 2018.
- [5] N. Wei, X. Lin, and Z. Zhang, "Optimal relay probing in millimeter-wave cellular systems with device-to-device relaying," *IEEE Trans. Veh. Technol.*, vol. 65, no. 12, pp. 10 218–10 222, Dec. 2016.
- [6] G. Yang and M. Xiao, "Performance analysis of millimeter-wave relaying: Impacts of beamwidth and self-interference," *IEEE Trans. Commun.*, vol. 66, no. 2, pp. 589–600, Feb. 2018.
- [7] S. Biswas, S. Vuppala, J. Xue, and T. Ratnarajah, "An analysis on relay assisted millimeter wave networks," in *Proc. IEEE ICC*, Kuala Lumpur, Malaysia, May 2016, pp. 1–6.
- [8] Y. Cai, Y. Xu, Q. Shi, B. Champagne, and L. Hanzo, "Robust joint hybrid transceiver design for millimeter wave full-duplex MIMO relay systems," *IEEE Trans. Wireless Commun.*, vol. 18, no. 2, pp. 1199–1215, Feb. 2019.
- [9] T. Bai and R. W. Heath, "Coverage and rate analysis for millimeter-wave cellular networks," *IEEE Trans. Wireless Commun.*, vol. 14, no. 2, pp. 1100–1114, Feb. 2015.
- [10] C. Skouroumounis, C. Psomas, and I. Krikidis, "Low-complexity base station cooperation for mmWave heterogeneous cellular networks," in *Proc. IEEE Globecom*, Washington, DC, Dec. 2016, pp. 1–6.
- [11] X. Yu, J. Zhang, M. Haenggi, and K. B. Letaief, "Coverage analysis for millimeter wave networks: The impact of directional antenna arrays," *IEEE J. Sel. Areas Commun.*, vol. 35, no. 7, pp. 1498–1512, July 2017.
- [12] S. Xu, N. Yang, and S. Yan, "Impact of load balancing on rate coverage performance in millimeter wave cellular heterogeneous networks," in *Proc. IEEE ICC Workshops*, Kansas City, MO, May 2018, pp. 1–6.
- [13] Y. M. Tsang and A. S. Y. Poon, "Detecting human blockage and device movement in mmWave communication system," in *Proc. IEEE Globecom*, Houston, TX, Dec. 2011, pp. 1–6.
- [14] A. Thornburg and R. W. Heath, "Capacity and coverage in clustered LOS mmWave ad hoc networks," in *Proc. IEEE Globecom*, Washington, DC, Dec. 2016, pp. 1–6.
- [15] H. Elshaer, M. N. Kulkarni, F. Boccardi, J. G. Andrews, and M. Dohler, "Downlink and uplink cell association with traditional macrocells and millimeter wave small cells," *IEEE Trans. Wireless Commun.*, vol. 15, no. 9, pp. 6244–6258, Sept. 2016.
- [16] F. Baccelli and B. Baszczyszyn, *Stochastic Geometry and Wireless Networks: Volume I Theory*. Hanover, MA: Now Publishers, 2009.
- [17] E. Turgut and M. C. Gursoy, "Coverage in heterogeneous downlink millimeter wave cellular networks," *IEEE Trans. Commun.*, vol. 65, no. 10, pp. 4463–4477, Oct. 2017.
- [18] S. Singh, M. N. Kulkarni, A. Ghosh, and J. G. Andrews, "Tractable model for rate in self-backhauled millimeter wave cellular networks," *IEEE J. Sel. Areas Commun.*, vol. 33, no. 10, pp. 2196–2211, Oct. 2015.
- [19] A. Thornburg, T. Bai, and R. W. Heath, "Performance analysis of outdoor mmWave ad hoc networks," *IEEE Trans. Signal Process.*, vol. 64, no. 15, pp. 4065–4079, Aug. 2016.
- [20] M. Haenggi, "Diversity loss due to interference correlation," *IEEE Commun. Lett.*, vol. 16, no. 10, pp. 1600–1603, Oct. 2012.